Audio Engineering Society

Conference Paper

Presented at the 2022 International Conference on
Automotive Audio
2022 June 8–10, Dearborn, MI, USA

A Simulation Environment to Evaluate the Effect of Secondary Source Coupling for Noise Reduction in an Automotive Application

Akshay Jagadish Khatokar[1], Samira Mohamady[1], and Allahyar Montazeri[2]

[1]*Department of Infotainment Systems and Functions (TV-I5), IAV Gmbh, Munich, Germany*
[2]*Engineering Department, Lancaster University, LA14YW, Lancaster, UK*

Correspondence should be addressed to Samira Mohamady, Allahyar Montazeri
(samira.mohamady@iav.de,a.montazeri@lancaster.ac.uk)

ABSTRACT

Passenger comfort has always been of pivotal importance in the interior design of an automobile. A critical aspect in reaching this goal in the automotive industry is the design and implementation of an effective active sound management system with the ability to personalize the acoustic environment inside the car. This, in turn, requires designing an active noise control (ANC) system to mitigate the unwanted noise and an active sound profiling system to implement the desired sound. Due to the complexity of the sound field inside the car cabin, having a high-fidelity model that reflects all details is a challenging task. Therefore, in this paper, we develop a simulation platform to be able to evaluate the performance of the ANC system and the distribution of the sound field as a result of this mechanism. This helps to get a better insight into the behaviours of the sound field inside the cabin before its actual implementation. One important feature of this model, which may also have a significant effect on the performance of the ANC system, is the inclusion of a full-scale numerical model of the loudspeaker. The realistic model of the loudspeaker developed in this way allows to model the effect of loudspeaker coupling in an enclosed space and investigate its effect on the ANC system. The model is compared against the simplified mathematical model of the enclosure developed in the previous work by the authors to see how the approximate geometry and simplified model of the loudspeaker would degrade the performance of the ANC system and measure the changes in the acoustic radiation impedance of the loudspeaker.

1 Introduction

As the need for fuel-efficient cars increased, the demand for lightweight structures grew significantly. This resulted in the generation of low-frequency noise because of the interaction between the road and the tyres of the car. It is a fact in noise control engineering that the curtailment of low-frequency sound below 1 kHz requires formidable effort due to its long wavelength at lower frequencies which would require the use of thicker absorption material to attenuate the noise. Especially in the automotive sector, this challenge continues to grow significantly as a result of multiple noise sources such as in-cab booming noise between 20 Hz–

300 Hz, which excites the structure of the car, noise due to the engine in the passenger cabin and as the demand for lightweight structures for fuel efficiency and quieter cabins for passenger comfort take to priority. One such concept to control the low-frequency noise was the introduction of the active noise cancellation (ANC) mechanism. This concept, introduced first by Paul Lueg in Germany in 1932, has found its vast utility today in a variety of applications such as noise cancellation headphones [1, 2] noise control of air conditioning ducts [3], active mufflers [4, 5] to name a few. The basic principle behind this mechanism is that of the superposition of sound waves to attenuate the noise. The superposition of sound waves induces destructive interference, which helps attenuate the noise.

The implementation of this modern concept of noise reduction in the three-dimensional spaces has been bounded as a result of its physical limitations, specifically, its unstable behaviour, the requirement of a significantly large gain controller and spatial mismatch [6]. There has been a considerable amount of research, and practical work carried out in the field of ANC technology and its real-world implementation. The experimental ANC set-up comprises both the structure and acoustic elements and their active interaction. This makes it extremely difficult to model the ANC mechanism directly into the real-world environment as it would be unpredictable, time-consuming and expensive as the behaviour of the environment would be unknown. To eliminate these limitations and to have an idea of the implementation environment, numerical modelling and simulations were introduced.

Over the years, analytical, numerical and experimental methods have been described for the implementation of the ANC [7]. For attenuation of the low-frequency noise caused by various factors such as engine noise and structure-borne noise, the use of a multi-channel ANC system in combination with an audio system was studied with the help of simulations and experimental set-ups inside the car cabin [8, 9]. With the advancement in computer technology and its capabilities, multiple simulation software has become stronger and more reliable over the course of time. This resulted in a strong emphasis on simulating the ANC mechanism before its actual implementation in the physical world. It involved the numerical modelling of the physical space, which plays an integral part in achieving ANC control over the low-frequency noise. The numerical modelling of the physical domain in most cases was carried out using methods such as Finite Element Method (FEM) [10], Boundary Element Method (BEM) [11, 12], Finite Difference Time Domain method (FDTD) [13, 14]. There has not been much work on implementing ANC with the help of the Finite Element Method (FEM) and Boundary Element Method as a coupled method. This paper focuses mainly on numerical modelling of a framework for the simulation of the ANC mechanism in a three-dimensional space with the help of the finite- and boundary element methods (FEM-BEM).

A detailed analysis of the acoustic environment and the study of the effect of multiple loudspeakers and microphones inside a confined enclosure has been carried out by Montazeri [15, 16]. It has been described and proven mathematically that when two or more loudspeakers work in a closed environment, the coupling of loudspeakers happens through the acoustic modes of the enclosure. However, the effect of loudspeaker coupling on the performance of the ANC system in an enclosed environment is investigated in several studies in [17, 18]. Both numerical and analytical results presented in [19] show that the coupling effect of the multiple loudspeakers will not change the amount of potential energy reduction in the enclosure. Nevertheless, this will undoubtedly alter the radiation impedance of each loudspeaker, it's volume velocity and hence the amplitude and phase of the voltages applied to the loudspeaker will change. This finding is also utilised to find the optimum position for loudspeakers and microphones in a rectangular enclosure in [20].

In this paper, we are extending the results in [19] by developing a high fidelity model for both loudspeakers and the acoustic environment. The effects of loudspeaker coupling are also presented.

2 Simulation Environment

The simulation of the ANC platform involves the electrical, mechanical and acoustic domains coupled with one another, as illustrated in Fig .1. Acoustic transfer paths are computed between the sound sources and the listening positions to enable the functioning of the ANC mechanism. In order to develop a framework to simulate the ANC mechanism, loudspeakers and listening positions are modelled in the numerical modelling software to replicate the real-world environment. Care is taken to model the parameters of the loudspeaker structure and its functionality as close as possible to that of

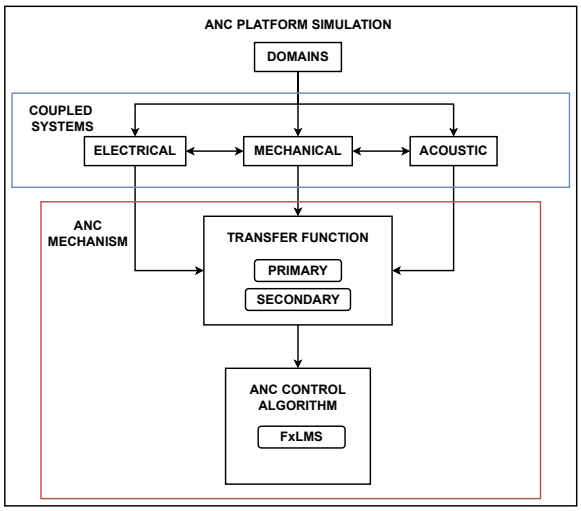

Fig. 1: ANC platform.

the actual loudspeaker itself. Section 2.1 and 2.2 describe the modelling and simulation of the loudspeaker driver attached to an infinite baffle and in free space conditions, respectively. Section 2.3 elucidates the simulation of the loudspeakers in an enclosure and determination of the transfer paths between the loudspeakers and the receiving positions. Section 3 describes the coupling of multiple loudspeakers when placed inside a closed environment. The paper is finally summarised and concluded in Section 4.

2.1 Simulating the Loudspeaker Driver

To start with, it is of utmost importance to numerically model and simulate the actual loudspeaker system before proceeding with the design of the ANC framework. This helps determine if the results of the numerically modelled loudspeaker are in good understanding with the actual loudspeaker system. For the purpose of simulation of the ANC mechanism, loudspeakers manufactured by Musikelectronik Geithain GmbH are considered. The model contains the geometry information of membrane, surround, spider, dust cap, voice coil former that includes the voice coil and the material components of the other individual components. The designed loudspeaker driver is circular in shape and has n-degrees of freedom (n–DOF), which must be computed. The concept of symmetry has been applied along its diameter to simplify geometry modelling. This effectively reduces the number of degrees of freedom to half ($n/2$–DOF), thereby exponentially reducing the

Table 1: Loudspeaker parameters used for numerical modelling.

Loudspeaker parameter	Value
Loudspeaker resistance	6.55 Ω
Loudspeaker inductance	0.384 H
Magnetic flux density × coil length	9.5971 $T.m$
Loudspeaker mass	0.02237 Kg
Loudspeaker damping	8.483
Closed box loudspeaker stiffness	3727.45 $N.m^{-1}$
Loudspeaker mechanical quality factor	2.2201
Loudspeaker electrical quality factor	0.3908
Loudspeaker total quality factor of loudspeaker	0.3323
Loudspeaker surface area	0.011866 m^2

computational cost [21]. Perfectly Matched Layers (PML) are used to simulate perfectly absorbing conditions without any refection of sound waves. This ensures the passing of the sound waves completely and helps prevent the occurrence of standing waves when simulated.

The electric input to the loudspeaker is given by an equivalent circuit under the electrical domain. Coupling between the mechanical and the electrical modules is related through magnetic flux density (B) and length of the conductor (L). The equivalent circuit is as presented in [22]. The force applied to the loudspeaker voice coil apex (f) is given by the Lorentz equation in Eq.1. The same has been modelled and simulated with the help of an electric module of the analysis software, paving the way for actual loudspeaker functionality. The Lorentz force is given as

$$f = BL \times i, \tag{1}$$

where i is the electric current in the loudspeaker circuit. The back induced voltage is fed into the circuit from the numerical model as the coil speed (u). The voltage source (V) achieves the coupling between the equivalent electric circuit and the mechanical domain. The induced voltage is given as:

$$V = BL \times u. \tag{2}$$

The loudspeaker membrane, dustcap, surround, and the air together accounts for the structure-acoustic coupling. The movement of the loudspeaker membrane

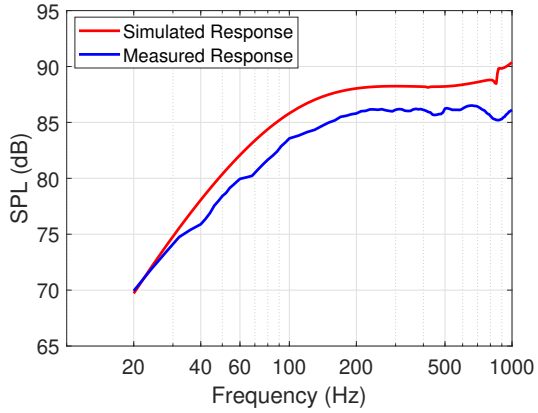

Fig. 2: SPL plot of the Loudspeaker driver.

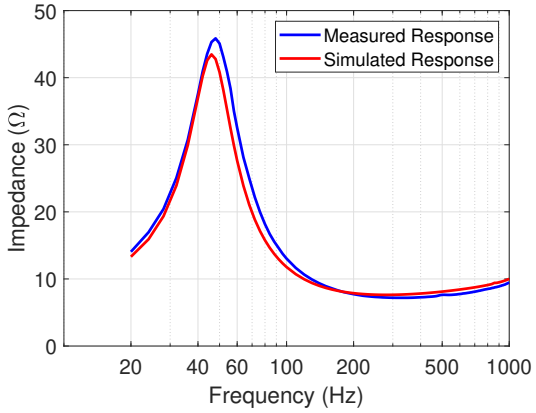

Fig. 3: Impedance plot of the Loudspeaker driver.

exerts a force on the surrounding acoustic medium. As the loudspeaker membrane has a very thin cross-section, it also experiences pressure over its membrane area due to the surrounding acoustic medium. This effectively accounts for a coupling interaction between the loudspeaker membrane and the latter over the surface area of the loudspeaker membrane, dustcap and the surround.

The simulation results are compared with actual acoustical and electrical measurements carried out with the help of a Clio12 measurement system consisting of the measurement hardware and software. The hardware system consists of the FW–02 interface and a corresponding measuring amplifier. A microphone is also coupled with the hardware system to carry out the corresponding acoustic measurements. The Clio12 standard software operates the above devices, which run on standard computer systems [23].

Fig. 2 shows the frequency response curve, and the impedance response curve of the simulation quite closely corresponds to that of the measurement curve. The simulated frequency response and the measured response show a very close resemblance and vary from each other by approximately 2 dB. The impedance response curve in Fig. 3 also exhibits similar characteristics between the simulated and the experimental measurement value. The simulated impedance value is found to be around 46 Hz with a corresponding value of 43.47 Ω and the measured impedance value is 45.86 Ω at 48 Hz.

2.2 Simulating the Loudspeaker Cavity

The design of the loudspeaker driver is encompassed in numerical modelling of a closed box loudspeaker in free space as shown in Fig. 4. The closed box design is modelled based on the TS parameters for the given loudspeaker model. The other components of the closed box loudspeaker are modelled as sound hard boundary walls and excluded from the analysis. As the design is symmetric about the length and width of the closed box loudspeaker, simulating only half the numerical model reduces the latter's number of degrees of freedom, thereby simplifying the numerical model and reducing the computation effort. This simplified model is solved in the frequency domain.

Fig. 5 confirms that the frequency response curve of the simulation quite closely corresponds to that of the measurement curve for a closed box loudspeaker. A sharp rise in the sound pressure level from around 280 Hz is observed in both the curves, which can be accounted to a phenomenon called 'baffle step'. A 'baffle step' is defined as the increase in the output of the loudspeaker as the size of the closed box enclosure becomes significant for a range of frequencies [24]. The sound waves begin to bounce off the wall at those frequencies. Fig. 6 manifests the impedance response for the simulation and measurement methods. Both trajectories tend to exhibit similar behaviour. The measured resonance frequency is 80 Hz and impedance of 46 Ω, while the simulated resonance frequency is 92 Hz and impedance of 43 Ω.

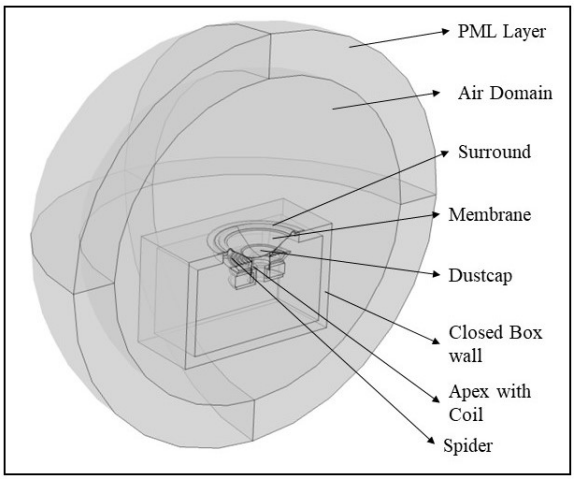

Fig. 4: Symmetric model of the Closed Box Loudspeaker.

Comparison between measurement and simulation data gives a better idea about validating the developed mathematical model. From this, it can be said that the developed simulation model for the loudspeaker driver and the closed box enclosure is valid.

2.3 Simulating the Loudspeaker in an Enclosed Space

To achieve the working of the ANC phenomenon over a closed acoustic space like a Sedan or SUV and to keep the simulation platform close to the actual environment of an automobile, the loudspeaker is modelled inside a simplified car shaped enclosure with dimensions representing the acoustic space inside an actual car cabin. Simple seat structures are modelled to resemble the cabin space of the car. The surface of the seat is considered to be leather and hence, it's respective acoustic property in terms of the complex valued impedance conditions are assigned to the surfaces of the seat structures based on the values obtained in reference [25]. The floor padding in cars is usually of the type tufted cut pile or loop-pile which usually has a synthetic latex base backing the primary fabric and the secondary fabric is then attached to make the carpet firm, and the roof trim in the cars is usually made up of polyester foam sheets and fiber-reinforced porous polymer sheets [26]. The acoustic property of the floor padding and the roof-trim is modelled as impedance boundary condition with high flow resistivity. The windows, front- and rear windshield are modelled with acoustic properties

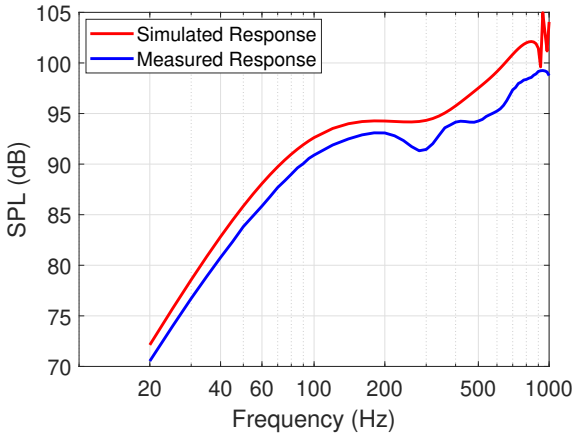

Fig. 5: SPL plot of the Closed box Loudspeaker.

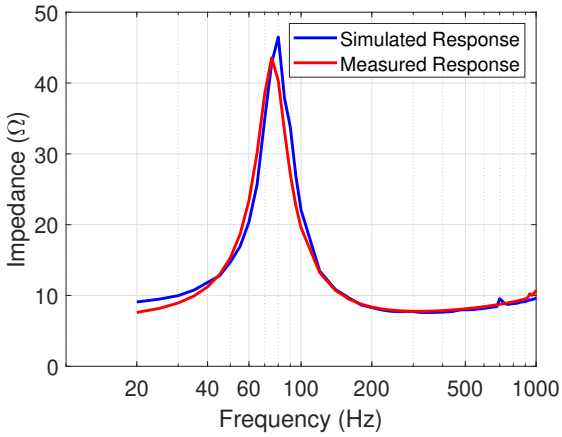

Fig. 6: Impedance plot of the Closed box Loudspeaker.

of glass, the dashboard and doors are assigned constant absorption coefficient with respect to the polypropylene material used in the manufacturing of actual cars.

The first eleven eigenfrequencies of the enclosure are tabulated in table 2. All relevant damping and absorption co-efficient of various structures of the car interior is presented in table 3. The closed box loudspeaker described in the above section is modelled along the length of the enclosure as shown in Fig. 7. The electrical input to the voice coil apex of the loudspeaker and the working of the loudspeaker is as described in the above section.

With an increase in the frequency range, the number of acoustic modes inside the enclosure increases. The

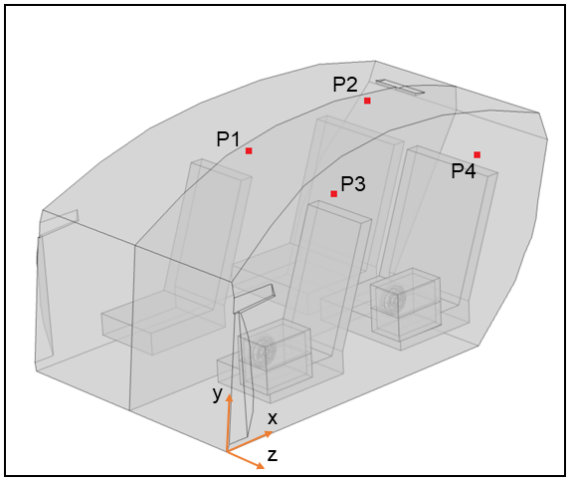

Fig. 7: Closed box loudspeakers placed inside the acoustic space of a car enclosure with receiving positions $P1$, $P2$, $P3$ & $P4$.

loudspeaker developed in the above section functions consistently well in the lower frequency region. Knowing that the engine noise and noise generated by the automobile structure are predominant in the lower frequency regime, a range between 20 Hz–200 Hz has been considered for simulation, study and calculations inside the enclosure. The complete numerical model is solved in the frequency domain.

2.4 Transfer Function Simulation

To achieve ANC at receiving positions inside a closed enclosure, the determination of the transfer paths become essential to relate between the output measured and the input being provided. This essentially comprises of two paths namely, the primary transfer path and the secondary transfer path. The same is applied to the mathematical model and simulations are carried out. The co-ordinate axes of the model and the complete simulation setup is as shown in Fig. 7. Four acoustic pressure probes $P1$, $P2$, $P3$ and $P4$ are modelled as receiving positions similar to those present in the front of the car and the rear of the car at coordinates (x = 0.85 m, y = 1.7 m, z = -0.7 m), (x = 1.75 m, y = 1.21 m, z = -0.7 m), (x = 1.05 m, y = 1 m, z = -0.3 m) and (x = 1.85 m, y = 1.1 m, z = -0.5 m), respectively, as in Fig. 7.

2.4.1 Primary Transfer Function

A primary noise source modelled in the form of a monopole sound source into the simulation model as

Table 2: Eigen frequencies of the enclosure.

No.	Frequency (Hz)
1	62.125
2	88.97
3	97.91
4	116.72
5	127.61
6	128.83
7	129.05
8	145.49
9	190.46
10	198.76
11	208.53

Table 3: Damping properties of the enclosure components.

Enclosure component	Type of Damping	Value
Door, Glass	Absorption co-efficient	0.01
Dashboard	Absorption co-efficient	0.005
Roof-top	Flow resistivity	20000 $Pa.s/m^2$
Carpet	Flow resistivity	10000 $Pa.s/m^2$
Seats	Impedance	max. 1 $Pa.s/m$

in Fig. 8. A primary sound source can be modelled as surfaces, edges or points. For simplicity, in this paper a point has been modelled as a primary sound source at (x = 0 m, y = 0 m, z = 0 m). The sound path between the noise source and the measuring positions in the enclosure are simulated. The path between the monopole noise source and the measuring position is called the primary transfer path. The SPL measured at positions $P1$, $P2$, $P3$ and $P4$ is shown in Fig. 9. The plot also contains the SPL recorded at the source location. The sharp rise in the SPL at 65 Hz, 90 Hz and 120 Hz can be accounted for effects of the eigenmodes present inside the enclosure in close proximity to the receiving positions at these frequencies. The transfer function calculated as the ratio of the output signal measured by the acoustic probe to the input signal provided to the loudspeaker acting as a noise source is called the primary transfer function. Fig. 10 shows the transfer function plot between the noise source and the measuring positions $P1$, $P2$, $P3$ and $P4$.

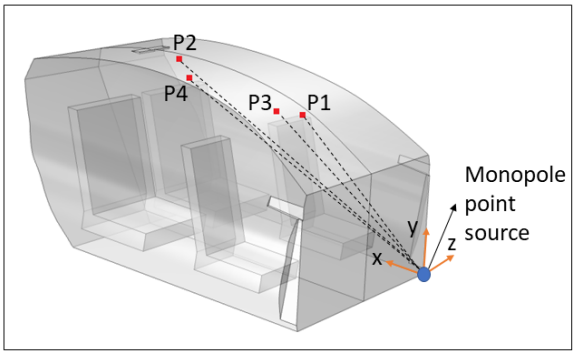

Fig. 8: Primary path comprising of the receiving positions and the modelled point source.

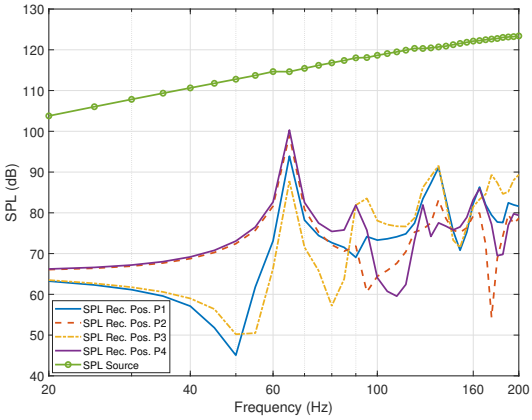

Fig. 9: Primary path SPL plot for the noise source and receiving positions $P1$, $P2$, $P3$ & $P4$.

2.4.2 Secondary Transfer Function

In Fig. 11, the path between the loudspeakers and the various measuring points defines the secondary transfer path, and the respective transfer function is calculated as the ratio of the output signal measured at the receiving positions to the signal input provided to the control loudspeaker. Two loudspeakers, one on the front door and the other on the car's rear door, are considered. The SPL is measured at positions $P1$, $P2$, $P3$ & $P4$ for individual loudspeakers working inside the enclosure and the plots are presented in Fig. 12 and Fig. 13. Individual secondary transfer paths is also computed between the above mentioned measuring positions, and each loudspeaker. The secondary transfer paths are computed by the operation of each loudspeaker individually at a given point in time. They are shown in Fig.

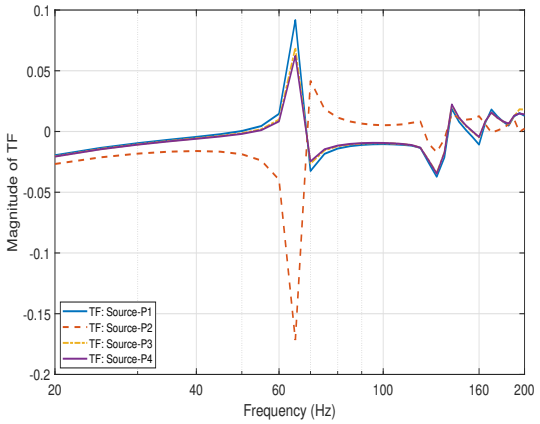

Fig. 10: Primary path transfer function between the noise source and listening positions $P1$, $P2$, $P3$ & $P4$.

14 and Fig. 15 corresponding to loudspeakers $LS1$ and $LS2$, respectively.

3 Coupling of Loudspeakers

In a closed acoustic environment as that of an automobile cabin, the coupling effect between two or more loudspeakers cannot be ignored, especially with a multi-input multi-output (MIMO) system. Coupling is a condition in which two or more sound emitting sources, when placed within a fraction of the wavelength, affect the radiation impedance of each other, thereby altering their working behaviour [17, 18, 19]. In this paper we consider the loudspeakers as described in Section 2.2 to simulate the coupling of the loudspeakers inside the enclosure.

Referring to the above-listed literature, the relation between acoustic pressure acting on the surface of each loudspeaker and its corresponding volume velocity is defined by the relation:

$$[SP_{\mathrm{L}}(\omega)]^{L\times 1} = [\mathbf{Z}_{\mathrm{c}}(\omega)]^{L\times L}\,[U_{\mathrm{L}}(\omega)]^{L\times 1}, \qquad (3)$$

where L represents the number of loudspeakers inside the enclosure, $SP_{\mathrm{L}}(\omega)$ is the net acoustic pressure on the surface of the L^{th} loudspeaker, Z_{c} is a symmetric coupling matrix with dimensions $\mathrm{L}\times\mathrm{L}$ and $U_{\mathrm{L}}(\omega)$ is the frequency dependent volume velocity generated by the L^{th} loudspeaker.The symmetric coupling matrix Z_{c}

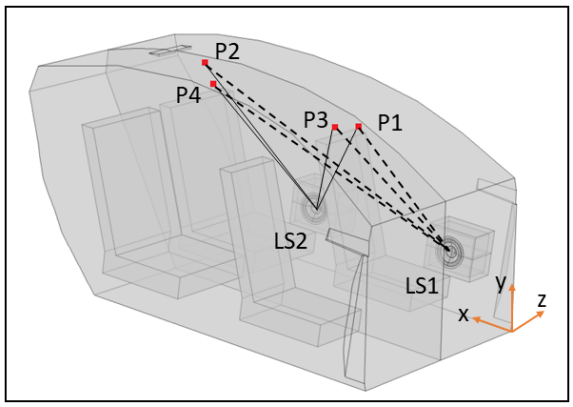

Fig. 11: Secondary path between loudspeakers 1 & 2 and receiving positions $P1$, $P2$, $P3$ & $P4$, respectively.

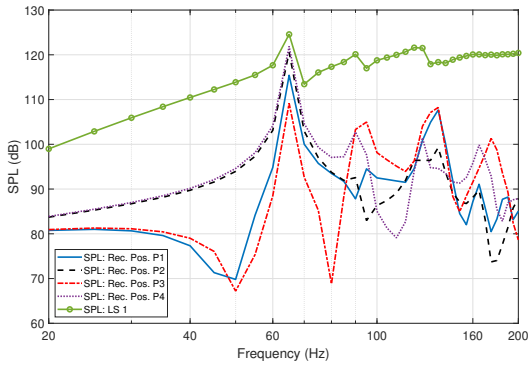

Fig. 12: SPL measured at receiving positions $P1$, $P2$, $P3$ & $P4$ when loudspeaker 1 is working independently.

is given by:

$$[\mathbf{Z}_{\mathrm{c}}(\omega)]_{ij} = \frac{\rho_0 c_0^2}{VS} \sum_{n=0}^{\infty} A_{\mathrm{n}}(\omega) \left[\int_{SP_i} \psi_{\mathrm{n}}(x,y_i,z)dxdz \right] \left[\int_{SP_j} \psi_{\mathrm{n}}(x,y_j,z)dxdz \right]. \quad (4)$$

Where i, j represent a set of two loudspeakers considered for coupling inside the enclosure, ρ_0 is the density of air, c_0 is the speed of sound in air, V denotes the volume of the enclosure, S is the surface area of the loudspeaker membrane, ψ_{n} represents the n$^{\mathrm{th}}$

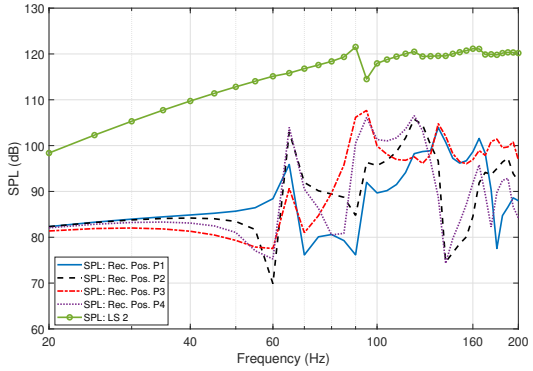

Fig. 13: SPL measured at receiving positions $P1$, $P2$, $P3$ & $P4$ when loudspeaker 2 is working independently.

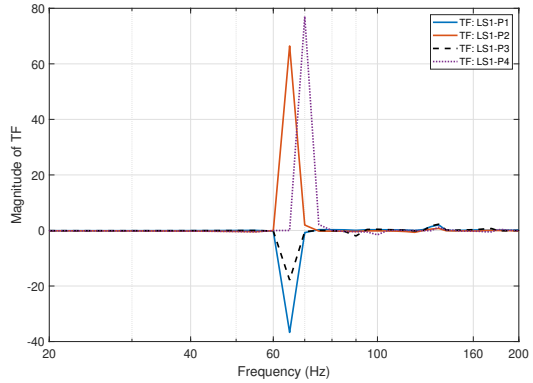

Fig. 14: Secondary path transfer function between the loudspeaker 1 and receiving positions $P1$, $P2$, $P3$ & $P4$.

acoustic mode of the enclosure, $A_{\mathrm{n}}(\omega)$ is the frequency dependant pressure amplitude and, x, y and z denote the coordinates of the loudspeakers placed inside the enclosure.

$$Z_{\mathrm{s}}(\omega)\left[U_{\mathrm{L}}(\omega)\right]^{1\times L} + \left[SP_{\mathrm{L}}(\omega)\right]^{1\times L} = Z(\omega)\left[V_{\mathrm{eL}}(\omega)\right]^{1\times L} \quad (5)$$

where $Z_{\mathrm{s}}(\omega)$ is the source strength matrix dependent on the volume velocity $U_{\mathrm{L}}(\omega)$ and $V_{\mathrm{eL}}(\omega)$ is the driving voltage applied across the terminals of the loudspeaker coil. As observed in Eq. 5, in a coupled environment, the volume velocity is not only affected

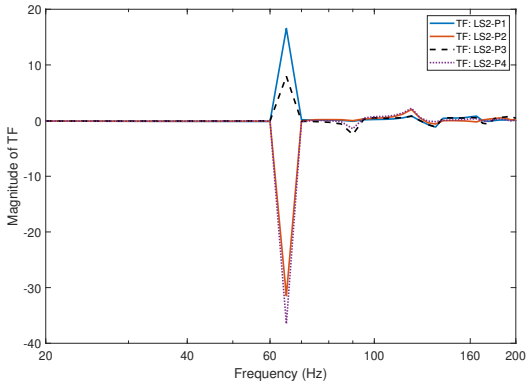

Fig. 15: Secondary path transfer function between the loudspeaker 2 and listening positions $P1$, $P2$, $P3$ & $P4$.

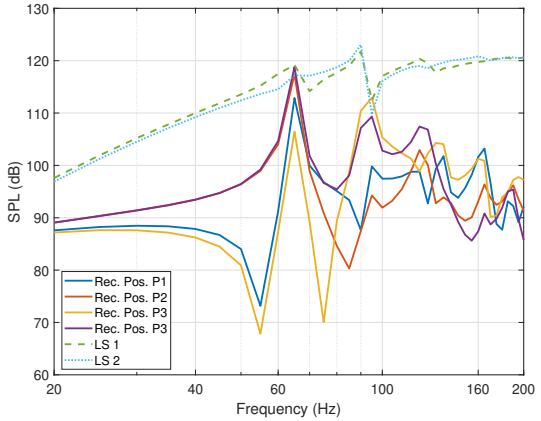

Fig. 16: SPL measured on the loudspeaker 1 & 2 surfaces and at receiving positions $P1$, $P2$, $P3$ & $P4$ for a coupled system.

by the driving voltages applied to the loudspeaker coils but also by the net acoustic pressure acting on the surface of the loudspeakers (SP_{L}). Considering a case where no voltage is applied across the loudspeaker coil terminals, the source strength is still driven by the influence of the acoustic pressure of the surrounding environment acting on the loudspeaker surface.

$$[U_{\mathrm{L}}(\omega)]^{1\times L} = \bar{Z}_{\mathrm{c}}(\omega)\,[V_{\mathrm{eL}}(\omega)]^{1\times L}, \tag{6}$$

where,

$$\bar{Z}_{\mathrm{c}}(\omega) = (Z_{\mathrm{c}}(\omega)I + Z_{\mathrm{s}}(\omega))^{-1}\,Z(\omega) \tag{7}$$

By writing the volume velocity of the acoustic sources in terms of their electrical voltages, it is possible to control the sound pressure inside the enclosure by considering the coupling of the loudspeakers. Eq. 6 denotes the relation between the coupled secondary sources and the driving voltage of the loudspeakers. It signifies the change in the driving voltages with respect to the coupling matrix $\bar{Z}_{\mathrm{c}}(\omega)$.

The voltage applied to each loudspeaker, the volume velocity generated over the loudspeaker, and the net acoustic pressure on the surface of each loudspeaker are obtained with the simulation of the numerical model. Relations 3 and 6 are used to find the complete transfer functions between the input voltage applied to the loudspeaker coil terminals of each loudspeaker to the output measured at the receiving positions.

The SPL inside the enclosure when two loudspeakers are working simultaneously as a completely coupled system is presented in Fig. 16. The effect of acoustic modes inside the enclosure is clearly visible in the case of coupling as well. A sharp rise in the SPL at 65 Hz can be accounted towards the corresponding loudspeaker resonant at that frequency. A sharp dip in the acoustic pressure inside the enclosure is measured at position $P2$ around 85 Hz. This may be due to the peak resonance of the enclosure and the associated zero at this frequency. The same phenomenon is also observed for the SPL measured at the position $P1$ at around 142 Hz.

The transfer function plot representing the coupling of two loudspeakers is shown in Fig. 17.

3.1 Effects of Loudspeaker Coupling

- **Variation of source strengths:** The source strength of each loudspeaker in the case of coupling and the uncoupled condition is presented in figure 18. As detailed in the paper by Montazeri [17, 18], when two or more sound sources are placed closed to each other, the strength of the sources varies due to the coupling effect between them. The difference between the coupled input voltage plot and the voltage plots when two loudspeakers are working individually can be clearly distinguished from the plot data. For an uncoupled system, the source strength is low compared to the coupled system response in the frequency range from 20 Hz up to 90 Hz and beyond this

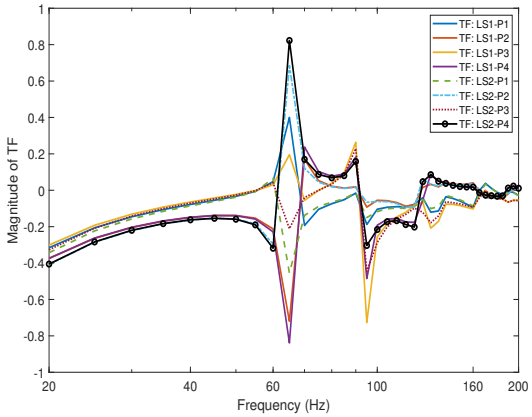

Fig. 17: Transfer function between the loudspeakers 1 & 2 and receiving positions $P1$, $P2$, $P3$ & $P4$, respectively for a coupled system.

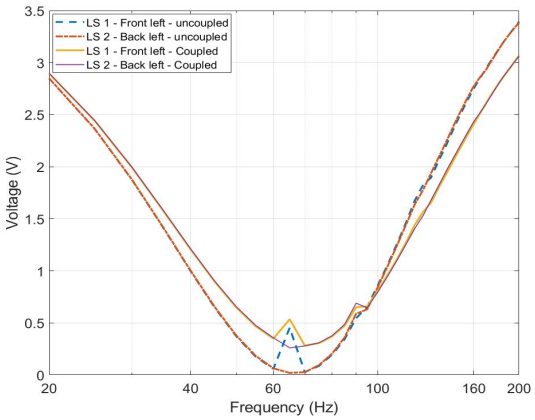

Fig. 18: Coupled system - Source strength variation of the loudspeakers.

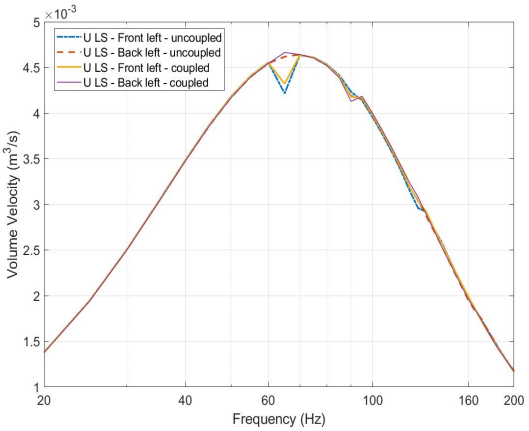

Fig. 19: Coupled system - Volume velocities generated by the loudspeakers.

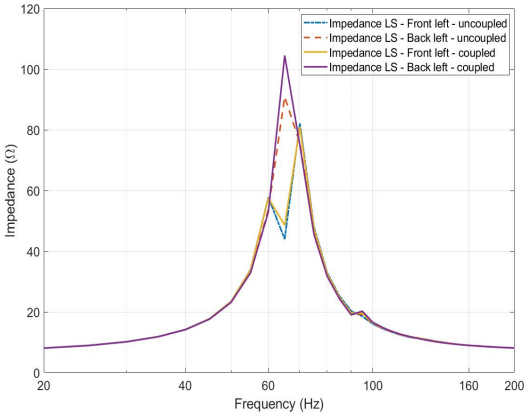

Fig. 20: Coupled system - Impedance response of the loudspeakers.

range, the source strength of the coupled system drops and that of the uncoupled system increases.

- **Variation of volume velocities:** The volume velocity over by a sound source is defined as the volume of fluid that passes through a given surface area per unit time once an acoustic pressure is generated by the source. Determination of the volume velocity over a sound source is important in determining acoustic parameters such as the source strength and transfer function analysis by using vibroacoustic coupling [27]. In this case, figure 19 represents the variation in the volume velocity over the two loudspeakers generated in the uncoupled cases when each loudspeaker is working independently inside the enclosure and in the case of coupling when both the loudspeakers are functioning together inside the enclosure. Comparing the plot data for the coupled and the uncoupled systems, it is observed that the volume velocities generated by each loudspeaker are relatively the same in both cases. But, for a coupled system, a slight variation in the volume velocity is observed at frequencies corresponding to the eigenmodes of the enclosure domain.

- **Variation of loudspeaker impedance:** With the

movement of the dynamic loudspeaker components, a vibroacoustic coupling is established. When two or more loudspeakers are working simultaneously in a closed environment, the net acoustic pressure acting on the surfaces of each loudspeaker causes a change in the loudspeaker impedance. The simulated results in figure 20 depict the same. The effects of coupling are visible in terms of the impedance of the loudspeakers. In comparison between a coupled and an uncoupled system, it is observed that due to the net acoustic coupling effect, the impedance value of the back-left loudspeaker is approximately 15 Ω greater than the impedance value measured when the system is uncoupled at a frequency of 65 Hz. For the front-left loudspeaker, the maximum impedance is observed at 70 Hz with not much difference in the impedance values between the coupled and the uncoupled system. It is also observed that there is a dip in the impedance at 65 Hz. This may be accounted to the acoustic mode of the enclosure cabin which passes over the back-left loudspeaker. With the above plot, it can be concluded that the first modes of the enclosure play a significant role in impacting the loudspeaker impedance compared to the other acoustic modes, where the impedance drops as the frequency range is increased.

From the above plots of source strengths and impedance variation of the loudspeakers, it can be concluded that under the first eigenfrequency of the enclosure, there is a high value of source strength in the form of the voltage applied to the loudspeaker terminals required for the functioning of the loudspeakers. This requirement of energy to drive the loudspeakers reduces as the frequency increases beyond the first eigenfrequency of the acoustic enclosure.

4 Summary

This paper presents a simulation platform for the implementation of the ANC mechanism in an enclosed space. The ANC simulation platform comprising of simplified and validated models of the closed box loudspeakers inside a mock-up car-cabin enclosure was simulated using the standard finite element method (FEM). An initial acoustic mode study was performed on the enclosure to estimate the behaviour of the acoustic pressure inside the enclosure due to its acoustic modes. Further, two loudspeakers were simulated inside the enclosure to study the coupling between them. In the automotive industry, the effects of the coupling of loudspeakers play a significant role in sound design. As the present industry works on the tuning of the audio systems to have a better perception, our research and study help tune the system based on energy in addition to the latter. Alongside the simulation of an ANC system in terms of noise attenuation, the developed simulation platform helps predict and optimize energy consumption.

References

[1] Song, Y., Gong, Y., and Kuo, S. M., "A robust hybrid feedback active noise cancellation headset," *IEEE transactions on speech and audio processing*, 13(4), pp. 607–617, 2005.

[2] Kuo, S. M. and Morgan, D. R., "Active noise control: a tutorial review," *Proceedings of the IEEE*, 87(6), pp. 943–973, 1999.

[3] Suzuki, D. and Kondo, K., "Application of ANC for singing voice attenuation," in *2014 IEEE 3rd Global Conference on Consumer Electronics (GCCE)*, pp. 63–64, IEEE, 2014.

[4] Kuo, S. M. and Nallabolu, S. P., "Analysis and correction of frequency error in electronic mufflers using narrowband active noise control," in *2007 IEEE International Conference on Control Applications*, pp. 1353–1358, IEEE, 2007.

[5] Sun, H., An, F., Wu, M., and Yang, J., "Experiments on performances of active-passive hybrid mufflers," in *Proceedings of the International Congress on Sound Vibration*, 2015.

[6] Gordon, R. T. and Vining, W. D., "Active noise control: A review of the field," *American Industrial Hygiene Association Journal*, 53(11), pp. 721–725, 1992.

[7] Esmailzadeh, E., Ohadi, A., and Alasty, A., "Multi-channel adaptive feedforward control of noise in an acoustic duct," *J. Dyn. Sys., Meas., Control*, 126(2), pp. 406–415, 2004.

[8] Sano, H., Inoue, T., Takahashi, A., Terai, K., and Nakamura, Y., "Active control system for low-frequency road noise combined with an audio

system," *IEEE Transactions on speech and audio processing*, 9(7), pp. 755–763, 2001.

[9] de Diego, M., Gonzalez, A., Ferrer, M., and Piñero, G., "Multichannel active noise control system for local spectral reshaping of multifrequency noise," *Journal of sound and vibration*, 274(1-2), pp. 249–271, 2004.

[10] Ohadi, A. and Emadi, A., "Active noise control simulation in a passenger car cabin using finite element modeling," Technical report, SAE Technical Paper, 2005.

[11] Bai, M. R. and Chang, S., "Active noise control of enclosed harmonic fields by using BEM-based optimization techniques," *Applied Acoustics*, 48(1), pp. 15–32, 1996.

[12] Brancati, A., Aliabadi, M., and Mallardo, V., "A BEM sensitivity formulation for three-dimensional active noise control," *International journal for numerical methods in engineering*, 90(9), pp. 1183–1206, 2012.

[13] Aslan, F. and Paurobally, R., "Modelling and simulation of active noise control in a small room," *Journal of Vibration and Control*, 24(3), pp. 607–618, 2018.

[14] Ospel, M. W., Werner, P., Wurm, F. H., and Witte, M., "Simulation of active noise control using transform domain adaptive filter algorithms linked with the inhomogeneous Helmholtz equation," *Applied Acoustics*, 182, p. 108250, 2021.

[15] Montazeri, A., Poshtan, J., and Kahaei, M. H., "Analysis of the global reduction of broadband noise in a telephone kiosk using a MIMO modal ANC system," *International Journal of Engineering Science*, 45(2), pp. 679–697, 2007.

[16] Montazeri, A. and Poshtan, J., "Optimizing a Multi-channel ANC System for Broadband Noise Cancellation in a Telephone Kiosk Using Genetic Algorithms," *Shock and Vibration*, 16(13), pp. 241–260, 2009.

[17] Montazeri, A. and Poshtan, J., "Modeling of coupling of loudspeakers for ANC system in a confined space," in *2008 International Conference on Electronic Design*, pp. 1–7, IEEE, 2008.

[18] Montazeri, A., Poshtan, J., and Poshtan, M., "Analysis of the Behavior of Coupled Loudspeakers in a MIMO ANC System in an Enclosure," in *2010 IEEE International Conference on Control Applications*, pp. 228–233, IEEE, 2010.

[19] Montazeri, A. and Taylor, C. J., "Modeling and analysis of secondary sources coupling for active sound field reduction in confined spaces," *Mechanical Systems and Signal Processing*, 95, pp. 286–309, 2017.

[20] Montazeri, A. and Poshtan, J., "GA-based optimization of a MIMO ANC system considering coupling of secondary sources in a telephone kiosk," *Applied Acoustics*, 70(7), pp. 945–953, 2009, ISSN 0003-682X.

[21] Jeff Gardiner, X. E. . C. P., "Using Symmetry To Reduce FEA Runtime," `https://www.xceed-eng.com/reducing-fea-runtime-with-symmetry/`, 2017, accessed: 2022-05-27.

[22] Ortiz, S., Kolbrek, B., Cobo, P., González, L. M., and Colina, C. d. l., "Point source loudspeaker design: Advances on the inverse horn approach," *Journal of the Audio Engineering Society*, 62(5), pp. 345–354, 2014.

[23] D'Appolito, J., "Measuring Loudspeaker Low-Frequency Response," *Audiomatica, Available: http://www. audiomatica. com*, 2018.

[24] Products, E. S., "Baffle Step Compensation," `https://sound-au.com/bafflestep.htm`, 2001, accessed: 2022-03-15.

[25] Didier, P., "In situ estimation of the acoustic properties of vehicle interiors, M.Sc. thesis," Technical report, DTU Electrical Engineering, 2019.

[26] Kumar, R. S., *Textiles for industrial applications*, CRC Press, 2013.

[27] Lee, J.-S. and Ih, J.-G., "On the method for estimating the volume velocity of an acoustic source in a chamber," *Journal of sound and vibration*, 182(4), pp. 505–522, 1995.